RSCPublishing   Faraday Discussions

FD 177: The free-energy barrier to hydride transfer across a dipalladium complex

SCHOLARONE™
Manuscripts

Journal Name

ARTICLE

The free-energy barrier to hydride transfer across a dipalladium complex

C. R. Vanston,[a] G. J. Kearley,[b] A.J. Edwards,[b]† T. A. Darwish,[b] N. R. Desouza,[b] A. J. Ramirez-Cuesta,[c] and M. G. Gardiner,*[a]

We use density-functional theory molecular dynamics (DFT-MD) simulations to determine the hydride transfer coordinate between palladium centres of the crystallographically observed terminal hydride locations, Pd-Pd-H, originally postulated for the solution dynamics of the complex *bis*-NHC dipalladium hydride [{(MesIm)$_2$CH$_2$}$_2$Pd$_2$H][PF$_6$], and then calculate the free-energy along this coordinate. We estimate the transfer barrier-height to be about 20 kcal mol^{-1} with a hydride transfer rate in the order of seconds at room temperature. We validate our DFT-MD modelling using inelastic neutron scattering which reveals anharmonicity of the hydride environment that is so pronounced that there is complete failure of the harmonic model for the hydride ligand. The simulations are extended to high temperature to bring the H-transfer to a rate that is accessible to the simulation technique.

Introduction

Transition metal hydrides are used or invoked as intermediates in a wide range of roles in catalysis and molecular hydrogen activation and storage, with compounds ranging from mononuclear complexes with single hydride ligands to large catalyst clusters or surfaces designed for hydrogen capture.[1-9] As well as providing an alternative to traditional catalytic cycles based on mononuclear complexes, some clusters are known to act as reservoirs for active mononuclear species.[10] The compound studied in the present work, [{(MesIm)$_2$CH$_2$}$_2$Pd$_2$H][PF$_6$], denoted MesPdH throughout this paper, is of interest in relation systems where partially reduced precatalysts/catalysts function either as reservoirs for active mononuclear catalysts, as noted above, and/or intermediates prior to larger cluster formation that eventually lead to inactive metal deposits in ethylene/carbon monoxide polymerisation.[11,12]

One important aspect of metal hydride chemistry is the ability of hydride ligands to undergo fluxional processes while remaining coordinated to the metal centre, a property that is useful to some catalyst activity and selectivity. Catalysts of this type may range from long established systems such as Wilkinson's catalyst for alkene hydrogenation[13] to multinuclear clusters with known or potential use for the catalysis of hydrogen transfer reactions.[14,15]

Solution ^{1}H NMR spectroscopic studies of MesPdH suggested the occurrence of a fluxional process, which was thought to involve the hydride ligand exchanging between the palladium centres (Figure 1). A major objective of the current study is to examine if the same process could occur in the solid state.
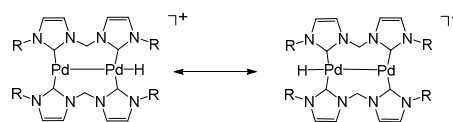

Figure 1. Proposed solution phase dynamics of MesPdH hydride transfer in [{(MesIm)$_2$CH$_2$}$_2$Pd$_2$H][PF$_6$], R= 2,4,6-trimethylphenyl.

Previous experimental studies on palladium hydride clusters have shown/suggested that hydride transfer processes between metal centres can occur either with the Pd-Pd bond remaining intact, or with cleavage of the Pd-Pd via a Pd-H-Pd geometry.[14-15] These studies are mostly based on the interpretation of solution phase fluxionality investigated by variable temperature NMR spectroscopy. The presence of good NMR probes in the clusters, phosphine ligands, can be invaluable in discriminating between mechanistic pathways. In the present case, we have no

experimental evidence for such detail of the hydride ligand transfer process. We note, however, that in this investigation of the H-transfer in the solid state, the more significant changes to the cluster core expected to accompany cleavage of the Pd-Pd bond in a linearly bridged Pd-H-Pd structure is likely to be disfavoured in the solid state due to crystal packing effects. In initial calculations on H-transfer in MesPdH it was revealed that it would be too slow to observe the H-transfer process directly, using for example quasielastic neutron scattering, so simulation at high temperatures seemed to be a possible way forward.

It is straightforward using DFT-MD to show that the dynamics of the H-ligand in MesPdH is largely determined by the time-dependent free-energy landscape of neighbouring molecular groups. These dynamics can be scaled up by increasing the temperature, and it turns out that 1500K a H-transfer event can just be seen, within 8ps, but that higher temperatures and longer times lead to destruction of the model. The central question is: is it only the amplitude of the fluctuations in the H-transfer free-energy surface that increase with temperature, or is a new process activated? We will show that the former case applies here, and a validation of the model at low temperature should still apply reasonably well at high temperature.

There are three difficulties to overcome with this strategy. Firstly, MesPdH, particularly in the full crystal structure, has a formidable number of degrees of freedom, but we are only interested in those that involve the H-ligand. The associated vibrational dynamics of this ligand can be conveniently studied almost in isolation by the use of inelastic neutron scattering (INS). Because the H-nucleus has a uniquely high incoherent neutron scattering cross-section, selective deuteration of all H-atoms, except the H-ligand, makes this ligand's vibrations more pronounced in the INS spectrum. Secondly, because the transfer process involves bond-making and breaking, and the general lack of a suitable force-field for MesPdH, we need to use DFT-MD. This method has the advantage of removing ambiguity, but is vastly more computationally expensive than empirical force-field methods, and consequently the size of the model and the time-scale covered will be rather limited. Finally, the unit-cell of the crystal is large and it is important to establish how the crystal forces may distort the gas-phase molecular conformation. It turns out that these solid-state effects are rather small and that the calculated vibrational dynamics of the isolated molecule and the full periodic crystal are very similar.

This paper is therefore primarily concerned with dynamics of the isolated MesPdH molecules and two of its selectively deuterated isotopomers illustrated in Figure 2. We retain MesPdH to denote the isotopically normal material, and use DMesPdD and DMesPdH for the fully deuterated and protonated hydride, respectively.
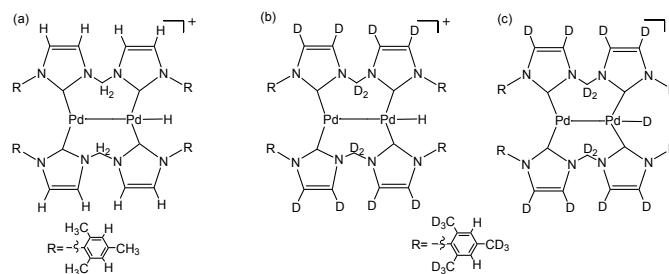

Figure 2. Deuterated isotopomers of MesPdH: (a) MesPdH (b) DMesPdH (c) DMesPdD. The ring H-atoms of the R groups could not be deuterated, but these are the same in b and c and so will contribute equally to the INS spectra.

Experimental

The complex MesPdH was synthesised using literature methods.[11] Handling of air-sensitive chemicals was carried out in a dry glove box (Innovative Technologies) under a nitrogen atmosphere with Schlenk type glassware.

Preparation of selectively deuterated samples for TOSCA

20 g of the ligand precursor *N*-2,4,6-trimethylphenyl imidazole (denoted MesIm) was provided to the National Deuteration Facility at ANSTO for chemical deuteration. This was achieved by heating the compound at 150 °C for 3 days under pressure in deuterium oxide in the presence of a mixture of Pt/C and Pd/C catalysts and using 20% v/v THF as a co-solvent[16]. The hydrothermal reaction mixture was purified on a silica column chromatography to give deuterated MesIm (96% yield) where the two phenyl protons remained essentially un-exchanged. Conversion to the deuterated diimidazolium salt using literature procedures[17] with deuterated dibromomethane (99% D) resulted in overall molecule deuteration of 84±2%. The deuteration percentages at each location of the molecule were calculated by ^{1}H and ^{13}C {^{1}H, ^{2}H} NMR spectroscopy, along with mass spectrometry and isotopic distribution analysis to confirm the specific site, as well as the overall isotopic purity respectively..

The deuterated imidazolium salt was then converted through previously reported methods[11] to the cationic dipalladium hydride DMesPdH Exchange of the hydride ligand to deuteride was accomplished by dissolving the relevant dipalladium hydride complex in deuterated methanol and stirring at 60°C for 2 days. Removal of the methanol under vacuum and subsequent redissolving and stirring in THF-*d₈* produced the deuterated THF solvate DMesPdD.

Instrumentation.

Inelastic neutron scattering spectroscopy was performed using the time-of-flight spectrometer TOSCA at the ISIS facility in Chilton, UK[18]. Approximately 1 g samples of the isotopomers shown in Figure 2 was available and in each case was placed in an aluminium sachet, which was cooled in a standard closed-

cycle cryostat. Spectral data were accumulated until an acceptable statistical quality was obtained at sample temperatures of 80 K and at 7 K. Data correction and transformation to the energy spectrum were made using standard local algorithms.

DFT calculations.

All DFT calculations were carried out using plane-wave code, Vienna Ab-Initio Simulation Package (VASP).[19-21] Isolated (or gas-pase) molecule calculations were performed on an isolated $\{(MesIm)_2CH_2\}_2Pd_2H^+$ cation composed of 117 atoms and contained in a periodic cell of dimensions 25x18x18 Å. This cell is large enough to avoid fictive intermolecular interactions. Geometry optimization, vibrational dynamics, and MD simulations were made using the Projector Augmented Wave (PAW) potential[22] and the Perdew-Burke-Ernzerhof (PBE) exchange-correlation functional.[23] In all cases a single k-point was used (Γ-point) and for accurate calculations a 400eV energy cut-off, with an electronic-energy convergence of 1.0×10^{-5} eV. For all MD simulations the energy cutoff was reduced to 300eV and the electronic convergence to 1.0×10^{-4} eV, with a time step of 1fs being used. The crystallographic unit-cell volume is almost 7000Å^3 and contains over 700 atoms so only a limited number of calculations was possible at low precision to obtain an estimate of solid-state effects on the H-ligand dynamics.

Geometry Optimization

Geometry optimization was achieved by allowing the atoms to relax to their minimum energy positions. For the crystal simulation the values of the cell constants were constrained to the experimental values and the full symmetry of the crystal structure was maintained during this optimization. For the isolated molecule optimization the initial conformation was taken from the crystal and the relaxed with no symmetry constraints. The final molecular structure was very similar to the initial structure illustrating that the crystal forces only play a minor role in determining the molecular conformation. An energy-convergence criterion of 1.0×10^{-4} eV was used for the isolated molecule and 1.0×10^{-3} for the crystal.

Matrix method molecular vibrations.

Normal-mode vibrational frequencies and amplitudes were calculated for the molecule by obtaining the Hessian matrix using VASP with the same criteria as for the geometry optimization. Atoms were displaced in positive and negative Cartesian directions from the minimum-energy positions by 0.03 Å to determine the second derivatives of the energy. The INS spectrum was calculated from the frequencies and amplitudes using CLIMAX[24] applying the instrumental parameters from the TOSCA spectrometer. Spectra for all isotopomers were calculated using the same force-constants,

but with the appropriate atomic masses being used in the corresponding inverse kinetic-energy matrix.

DFT-MD Simulations

The matrix method uses the harmonic approximation, which turns out to be poor for vibrations of the H-ligand. Ab-initio MD allows exploring the form and origin of anharmonicity taking finite temperature of the sample into account, which is required not only for spectral agreement, but more importantly for the study of the H-transfer process. For all simulations a 4ps equilibration on the energy-minimized structure in the isokinetic ensemble at the target temperature was performed to distribute the kinetic energy within the system. For the periodic crystal model this was followed by 4.2ps production run in the microcanonical ensemble. For the isolated molecule models, an additional 4ps equilibration in the microcanonical ensemble was made followed by an 8.5ps production run. The MD trajectories from the low temperature runs were used to calculate the INS spectrum using nMoldyn[25]. This was achieved via the incoherent intermediate scattering function $F(Q,t)$ that was calculated on a regular grid in both momentum transfer, Q, and time, t, which was then Fourier transformed to obtain the scattering function $S(Q,\omega)$. The appropriate cut in Q,ω was taken to coincide with the experimental INS spectrum on TOSCA. This spectrum was then convoluted with the instrumental resolution function to obtain the calculated INS spectrum.

Results and Discussion

We will first describe the vibrational spectra of the MesPdH analogues and how these are interpreted using two different standard approaches. This provides a validation of the MD approach, and we then provide some justification for being able to extend this to much higher temperatures. This gives access to the H-transfer process that is seen a single time in the high-temperature DFT-MD simulation. The accessible free-energy profile is then analysed and extended to include the H-transfer.

Comparison of observed and calculated INS spectra.

The experimental INS spectra of DMesPdD and DMesPdH are remarkably similar, as illustrated in Figure 3. The expectation from the matrix-method calculation, is that the H-ligand present in DMesPdH would produce a strong feature in the 50 meV region corresponding to an out-of-plane wagging (H-Pd-Pd deformation), that would be absent in the spectrum of DMesPdD, as shown in the lower part of Figure 4. It is worth noting that in both analogues there are 2 un-exchanged H-atoms on each trimethylphenyl unit (see Figure 2) and these will contribute extra peaks from vibrations of the organic ligands, but these are the same for both analogues.
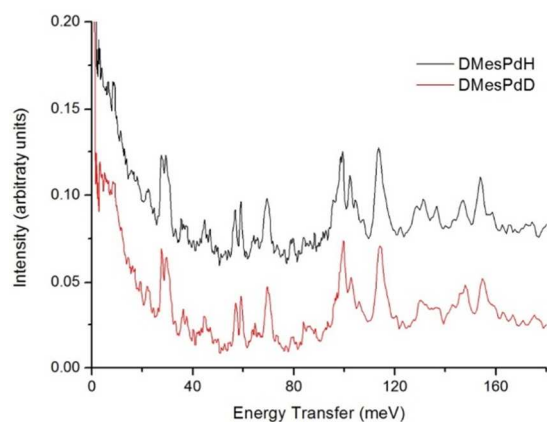
Figure 3. Comparison of INS spectra for DMesPdH and DMesPdD obtained at TOSCA. Relative intensity shifted for clarity. Note the strong similarity between these spectra despite the isotopic difference of the H(D) ligand
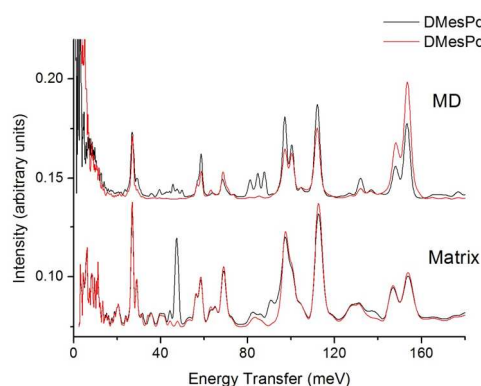

Figure 4. Comparison of the calculated spectra of DMesPdH and DMesPdD by MD and Matrix simulation methods. These spectra should also be compared with the experimental spectra in figure 3. Relative intensities shifted for clarity.

The absence of the strong peak at around 50meV predicted by the matrix method is due to a breakdown of the harmonic approximation for modes of the H-ligand. This is easily demonstrated by using the alternative MD method to produce the calculated INS spectrum. Whilst DFT-MD lacks proper treatment of overtones and combinations, it has the advantage that it makes no assumption about the form of the vibrational (or other) potential. The result shown in the upper part of figure 4 is that the strong peak at 50 meV is indeed absent in the calculated spectrum, and even a casual examination of the MD trajectories for the H-ligand show the dynamics to be locally diffusive rather than oscillatory. Normally the difference between the INS spectra calculated by the two methods is small, and even the differences in figure 4 between 80 and 100 meV that are in part due to the lack of overtones and combinations in the MD, would be considered as significant. To our knowledge, the difference at around 50meV in the current example is much larger than any reported so far.

The main aim of the current work is to study the H-transfer and the purpose of the INS is to validate that DFT-MD can at least reproduce the dynamics measured on the low-frequency part of the vibrational spectrum. We will take the general spectral agreement, and in particular the correct prediction of the non-oscillatory H-ligand dynamics, as a validation of the method.

MD at high temperature.

Computationally based energy-barrier calculations are generally performed by mapping the potential energy of the system as a function of some pre-defined reaction coordinate, taking no account of thermal motion. Even in better defined systems such as linear hydrogen bonds the involvement of many degrees of freedom can play a crucial role[26] so in MesPdH, where the H-atom is weakly bound and surrounded by molecular groups, each with many degrees of freedom, the choice of reaction coordinate is bewildering. The simple solution is to use MD to sample the free energy surface in a systematic and physically meaningful way, albeit at lower precision and greater computational expense. The difficulty is that the amplitudes sampled are limited by the available kinetic energy (simulation temperature). Increasing the MD simulation temperature should be more realistic than mapping potential-energies along pre-determined coordinates (at zero K), but it is still useful to provide additional justification.

We increased the simulation temperature until a transfer process occurred once within the timescale of the simulations (8ps). The crucial coordinate for the transfer process turns out to be the dihedral angle between plane of a heterocyclic ring and the Pd-H vector, which approximates to an extension of the mode that was incorrectly predicted by the harmonic approximation at 50meV in the INS. The actual definition used is shown in Figure 5a, but for convenience we will refer to this as Pd-Pd-H, to which it approximates. Clearly, this coordinate is not a normal coordinate of the system and so has a distributed spectral profile, which is shown (from the MD simulations) in Figure 5b. The crucial point illustrated in this figure is that this frequency distribution does not change significantly between 50K, where this is validated against experiment, and 1500K where the transfer was seen in the MD, although there is a large increase in amplitude. A limited MD simulation for the periodic crystal at 300K shows a very similar profile in Figure 5b to those of the isolated molecule. This indicates than not only are the vibrational dynamics dominated by intra-molecular interactions, but also the H-transfer mechanism.
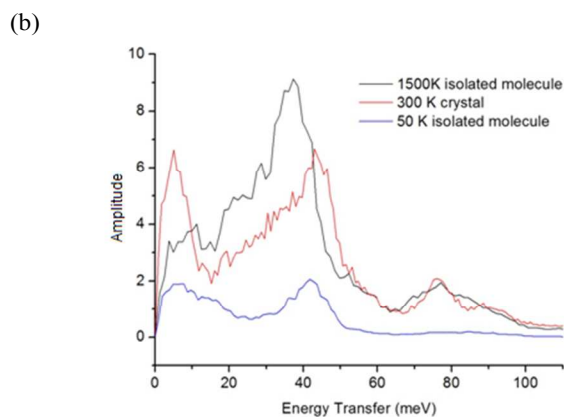
(a)

(b)
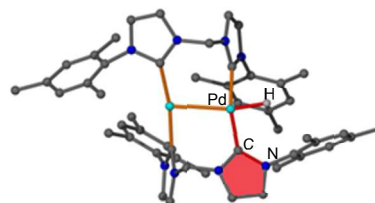
Figure 5. (a) Structure of the cation of MesPdH indicating plane used to define the dihedral torsion coordinate. We do not actually use Pd-Pd-H, although we denote it this way in the text, because that coordinate includes motion of both Pd atoms. (b) Frequency spectra of the hydride torsion showing comparison between the isolated molecule at 1500 K and 50 K, as well as with the periodic structure calculation. Note that other than the lattice modes below 10meV, there is little difference between the crystal and isolated models.

Hydride transfer energy barrier

The actual transfer process is almost certainly from terminal H at one Pd-atom, to bridging-H between the two Pd-atoms to terminal H at the second Pd-atom. We never observed this whole process, or the competing "bridge and return" process. The resources for the longer simulations required for this are not available to us and increasing the temperature destroys the model before any transfer process is seen. Consequently we base our analysis on the dihedral angle shown in Figure 5a. The temporal evolution of this Pd-Pd-H coordinate contains the resultant of the dynamics of the neighbouring ligands to which it is strongly coupled. To estimate the barrier to the transfer process the Pd-Pd-H angle we calculate the free energy from the frequency distribution of this angle during the 8 ps simulation at 1500K as:

$$FE_{(Pd-Pd-H)} = kT ln(\frac{P_{(Pd-Pd-H)}}{P_{(max)}})$$

(1)

Where T is the temperature of the simulation, $P_{(Pd-Pd-H)}$ is the time average population of a particular value of the angle, and P(max) is the maximum value of $P_{(Pd-Pd-H)}$. This energy function is shown in Figure 6. Because only a single transfer was seen during the simulation, there are no data around the peak of the barrier, and it would take an extremely long simulation to obtain these. In the absence of a known functional form we fit these angle-dependent data with a sinusoidal function resulting in an estimate for the energy barrier between 19 and 23 kcal mol^{-1}. By using the Arrhenius equation:

$$k = Ae^{\frac{-E_a}{RT}}$$

(2)

Where k is the rate constant, A is the rate pre-factor, E_a is the activation energy, R is the universal gas constant 1.986×10^{-3} kcal mol^{-1} K^{-1} and T is the temperature. The pre-factor was determined using the observed single transfer in the MD as the rate at 1500K, providing a room-temperature transfer rate of one transfer per 5.3 seconds. However, because the error in the barrier transforms exponentially to the rate, the limiting values are 360 ms and 77 s.
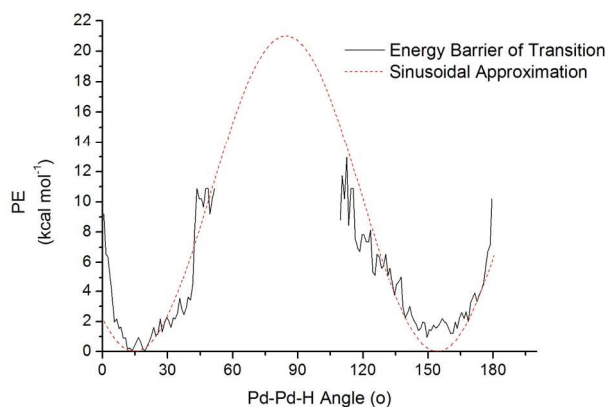

Figure 6. Free energy from the frequency distribution of the Pd-Pd-H angle approximated with a sinusoidal function to estimate the energy barrier.

We have made no attempt at this stage to analyse the correlations between torsional motions of the methyl groups, whole-body torsions of the ligands and the H-transfer process. These are clearly central to the H-transfer process and could be chemically tailored to either increase or decrease the rate, or indeed to trap the H-ligand in a bridging or terminal position.

Conclusions

Many studies have successfully used potential-energy mapping to obtain calculated dynamics that agree well with experimental results. This method ignores entropy, which enters in the current example through the highly flexible local environment of the H-ligand, and as we have shown, the mapping methods are then not appropriate. From a solid-state structural view the H-ligand is bonded as part of molecular solid, but from a dynamical view the H-atom experiences a more clathrate-like confinement, in which host-guest interactions inevitably dominate. The H-transfer process is correspondingly more diffusive in nature, broadly analogous to transport between different pores. The H-atom is held as much within the confines of the neighbouring ligands as by the closest metal atom, and our calculations show that the crystal forces have little effect on this environment, or the overall molecular conformation.

It is difficult to determine barriers to slow transfer processes in complex systems that have many degrees of freedom so we have attempted to circumvent this using approximations that may not be general, but are suitable for the system under study. In particular, we have used an MD simulation at a temperature that is high enough to see the H-transfer process within our resource-limited time, but even though this is above the decomposition temperature, it is low enough that this does not occur within the simulation period. In this way the MD probes physically meaningful coordinates and takes account of the dynamics of the whole system, albeit somewhat limited close to the actual transfer barrier. Additional MD simulations show that it is not the amplitude of the dynamics that lead to H-transfer, but rather a change their geometry, or the onset of a new process. At least for these transfer-coordinates it is reasonable to extrapolate the low-temperature INS validation to the higher temperature dynamics.

It would be difficult, but very interesting to measure this transfer process in the solid state experimentally. This would provide a strong incentive to put further effort into detailed understanding of the transfer process and the role of slow dynamics of the hydride environment.

Acknowledgments

Notes and references

[a] School of Physical Sciences (Chemistry), University of Tasmania, Private Bag 75, Hobart, Tasmania 7001, Australia.

[b] Bragg Institute, Australian Nuclear Science and Technology Organization, Locked Bag 2001, Kirrawee DC, NSW 2232, Australia.

[c] Oakridge National Laboratory-Chemical and Engineering Materials Division, PO Box 2008 MS6473, Oakridge TN 37831-6473.

† Presenting Author.

See DOI: 10.1039/b000000x/

1   N. K. Nag, *J. Phys. Chem. B*, 2001, **105**, 5945.

2   C. M. Hagen, L. Vieille-Petit, G. Laurenczy, G. Suss-Fink and R. G. Finke, *Organometallics*, 2005, **24**, 1819.

3   S. K.Brayshaw, A. Harrison, J. S. McIndoe, F. Marken, P. R. Raithby, J. E. Warren and A. S. Weller, *J. Am. Chem. Soc.*, 2007, **129**, 1793.

4   S. Chaudhuri, J. Graetz, A. Ignatov, J. J. Reilly and J. T. Muckerman, *J. Am. Chem. Soc.*, 2006, **128**, 11404.

5   M. Pérez Jigato, B. Coussens and D. A. King, *J. Chem. Phys.*, 2003, **118**, 5623.

6   F. Ozawa, H. Okamoto, S. Kawagishi, S. Yamamoto, T. Minami and M. Yoshifuji, *J. Am. Chem. Soc.*, 2002, **124**, 10968.

7   M. S. Viciu, G. A. Grasa and S. P. Nolan, *Organometallics*, 2001, **20**, 3607.

8   M. A. Zuideveld, P. C. J. Kamer, P. W. N. M. van Leeuwen, P. A. A. Klusener, H. A. Stil and C. F. Roobeek, *J. Am. Chem. Soc.*, 1998, **120**, 7977.

9   Y. Duan, L. Li, M. Chen, C. Yu, H. Fan and Y. Zhou, *J. Am. Chem. Soc.*, 2014, **136**, 7688.

10   M. Baya, J. Houghton, D. Konya, Y. Champouret, J. Daran, K. Q. A. Leñero, L. Schoon, W. P. Mul, A. B. van Oort, N. Meijboom, E. Drent, A.G. Orpen and R. Poli, *J. Am. Chem. Soc.*, 2008, **130**, 10612.

11   P. D. W. Boyd, A. J. Edwards, M. G. Gardiner, C. C. Ho, M. Lemee-Cailleau, D. S. McGuinness, A. Riapanitra, J. W. Steed, D. N. Stringer and B. F. Yates, *Angew. Chem. Int. Ed.,* 2010, **49**, 6315.

12   M. G. Gardiner, C. C. Ho, F. M. McKay, D. S. McGuinness and M. Tucker, *Dalton Trans.*, 2013, **42**, 7447.

13   S. B. Duckett, C. L. Newell and R. Eisenberg, *J. Am. Chem. Soc.*, 1994, **116**, 10548.

14   D. Evrard, K. Groison, Y. Mugnier and P. D. Harvey, *Inorg. Chem.*, 2004, **43**, 790.

15   C. Cugnet, D. Lucas, E. Collange, B. Hanquet, A. Vallat, Y. Mugnier, A. Soldera and P. D. Harvey, *Chem. Eur. J.*,2007, **13**, 5338.

16   T. A. Darwish, A. R. G. Smith, I. R. Gentle, P. L. Burn, E. Luks G. Moraes, M. Gillon, P. J. Holden and M. James, *Tetrahedron Lett.*, 2012, **53**, 931.

17   M. G. Gardiner, W. A. Herrmann, C. Reisinger, J. Schwarz and M. Spiegler, J. Organomet. Chem, 1999, **572**, 239.

18   Ramirez-Cuesta, A. J., Parker, S. F. and Tomkinson, J., in *TOSCA User Guide*.

19   G. Kresse and J. Furthmüller, *J. Comp. Mat. Sci*, 1996. **6**, 15.

20 G. Kresse and J. Hafner, *J. Phys. Rev. B*,, 1993, **47**, 558.

21   G. Kresse and D. Joubert, *J. Phys Rev. B*,, 1999, **59**, 1758.

22   P.E. Blochl, *J. Phys. Rev. B.*, 1994, **50**, 17953.

23   J.P. Perdew, K. Burke and M. Ernzerhof, *Phys. Rev. Let.*, 1996, **77**, 3865.

24 Kearley, G. J. *Nuclear Instrumental Methods*, 1995, **354**, 53.

25   Kneller, G. R., Keiner, V., Kneller, M. and Schiller, M. *Computer Physics Communications*, 1995, **91**, 191.

26 M. Plazanet, N. Fukushima, M. R. Johnson, A. J. Horsewill and H. P. Trommsdorff, *J. Chem. Phys.,* 2001, **115**, 3241.